Computational Materials Science 44 (2009) 1296–1306

Contents lists available at ScienceDirect

Computational Materials Science

journal homepage: www.elsevier.com/locate/commatsci

# Anharmonic analysis of defective crystals with many-body interactions using symmetry reduction

Shahram Kavianpour [1], Arash Yavari [*,2]

*School of Civil and Environmental Engineering, Georgia Institute of Technology, 790 Atlantic Dr., Atlanta, GA 30332, USA*

ARTICLE INFO

*Article history:*
Received 12 May 2008
Received in revised form 27 August 2008
Accepted 29 August 2008
Available online 19 October 2008

*Keywords:*
Lattice defects
Elasticity
Lattice statics
Symmetry reduction

ABSTRACT

In this paper we first classify and formulate various types of defects with respect to their symmetries and then show that with this general formulation, one can study the structures and energetics of defects in different crystalline materials effectively. We present all the calculations for the embedded-atom-type potentials but the formulation can, in principle, be applied for any many-body interatomic potential. As examples of defects in crystals with many-body interactions, we study point defects, free surfaces and grain boundaries in fcc Cu and grain boundaries in NiAl. We discuss free surface modelling by relaxing both a semi-infinite lattice and a slab with increasing finite thickness. We demonstrate through several numerical examples that our general framework of anharmonic lattice statics can be used for comparing different interatomic potentials in terms of the structure and energy they predict for a given defect. In the case of fcc Cu, we show how both the structures and energetics of different defects can strongly depend on the choice of potentials.



## 1. Introduction

In nature crystalline solids always have defects of different types. In other words, a mathematical crystal is, in general, an ideal configuration and in crystalline materials one can almost always find symmetry-breaking objects, i.e. defects, such as point defects, free surfaces, twin boundaries, dislocations, etc. Presence of defects in crystalline materials plays an important role in determining their physical, thermal and mechanical properties.

In the case of multi-scale simulation methods, atomistic simulations are restricted to a reduced domain. The exterior region to the atomistic domain is usually a continuum domain that surrounds the fine atomistic domain. There are two major types of coupled atomistic-continuum methods: (1) methods that explicitly use finite elements for the continuum domain, and (2) methods that use Green's function technique for the continuum domain to eliminate degrees of freedom associated with the exterior region. Among the works on the first type of coupled methods, the works by Kohlhoff et al. [62] and Tadmor et al. [87] can be mentioned.

To completely eliminate degrees of freedom associated with the continuum domain and directly model the atomistic region, a Green's function approach can be used. This type of coupled atomistic-continuum methods are often called the flexible boundary methods. Among such methods the work by Sinclair et al. [82], who introduced a flexible boundary method and applied it to a 2-D straight dislocation, and the work by Rao et al. [79], in which they extended this technique to study 3-D dislocation problems, should be mentioned. In some recent works [68], this method is used to derive a formulation for quasi-static multi-scale boundary conditions and then is applied to atomistic simulations [81]. Although in all these coupled atomistic-continuum methods of simulation of defects, the coupling of continuum region identifies a flexible boundary condition to the atomic-scale region and is intended towards a more accurate solution, a discrete method of solution for the core region with atomistic interactions also plays a key role in the solution. It is noteworthy to mention that in any partially symmetric defective crystal, both the atomistic and the continuum regions would naturally have the same symmetry and therefore, the dimension of both regions can be reduced similarly. In this paper, we are interested in a systematic formulation of the atomistic region and identification of a flexible boundary condition is not our objective. However, a flexible boundary condition can be applied to our method of simulation with coupling a continuum region exterior to the atomistic region.

Here, we formulate different types of defects in crystalline materials systematically using their symmetries to reduce the order of their corresponding governing difference equations and show the effectiveness of our formulation in several numerical examples. The idea of symmetry reduction in defective crystals has been known for a few decades and has been exploited in different solution methods for crystal defects. However, to our best

* Corresponding author. Tel.: +1 404 894 2436; fax: +1 404 894 2278.
*E-mail address:* arash.yavari@ce.gatech.edu (A. Yavari).
[1] Deceased.
[2] Research supported by the Georgia Institute of Technology.

0927-0256/$ - see front matter © 2008 Elsevier B.V. All rights reserved.
doi:10.1016/j.commatsci.2008.08.025

knowledge, this technique has not been systematically formulated for defective crystals.

The only available technique suitable for generating analytic and semi-analytic[3] solutions for defective crystals is the method of *lattice statics* [12]. In this paper, we present a formulation of lattice statics that is capable of semi-analytical modelling of defects in crystals with many-body interactions. As an example of many-body potentials, we work with embedded atom potentials, although any other interatomic potential can be treated similarly. We show how one can do semi-analytical lattice calculations for different types of defects. We also show that our lattice statics technique can be used as a tool for comparing different interatomic potentials in terms of the defect structures and energetics that they predict. Our major goals of working within this framework and its advantages are:

- Anharmonic lattice statics can be used to analyze the structures and energetics of different defects very efficiently and fast using symmetry conditions. Our method does not assume any periodicity and hence our calculations will be free of any spurious periodicity effects.
- This framework can be used as a tool for comparing different interatomic potentials in terms of the structures and energetics they predict for different defects. To our best knowledge, this has not been done systematically in the literature of computational physics.
- Modelling defective crystals as discrete boundary-value problems, one can learn certain details about a specific defect that may not be possible using purely numerical techniques. We will see this clearly in the case of free surfaces.
- In this paper, we are mainly interested in the static configurations of defects at $T = 0$ and will not consider any finite temperature effects. The appropriate method for studying the thermodynamics of defects at low temperatures is the method of lattice dynamics (see [63,92,2,3,74], and references therein). Establishing a framework for $T = 0$ calculations with a clear structure is a first step in thermodynamic analysis of defects at low temperatures, when MD cannot be used. Extension of the present work to finite temperatures will be the subject of a future communication.

This paper is organized as follows. In Section 2, given a reference configuration we find the linearized governing equations for a system of interacting particles with possible many-body interactions. Partial symmetry and symmetry reduction of the governing equations are also briefly discussed. In Section 3 we study several defect problems. We will discuss the solution methods and some subtleties in modelling these defects as discrete boundary-value problems. Conclusions are given in Section 4.

## 2. Defective crystals and symmetry reduction in a collection of atoms with many-body interactions

Consider a collection of atoms $\mathscr{L}$ with the current configuration $\{\mathbf{x}^i\}_{i\in\mathscr{L}} \subset \mathbb{R}^3$. We assume that, in addition to pairwise interactions, many-body interactions are also present. A large class of materials can be modelled by embedded atom (EAM) potentials [20] and hence we present our formulation for EAM-type potentials, however, without excluding other possibilities. For a system governed by an embedded-atom-type potential, the total energy of the collection $\mathscr{L}$ has the following form[4]

$$\begin{aligned}\mathscr{E}(\{\mathbf{x}^i\}_{i\in\mathscr{L}}) &= \mathscr{E}^{\text{pair}}(\{\mathbf{x}^i\}_{i\in\mathscr{L}}) + \mathscr{E}^{\text{cohesive}}(\{\mathbf{x}^i\}_{i\in\mathscr{L}})\\ &= \frac{1}{2}\sum_{\substack{i,j\in\mathcal{L}\\ j\neq i}} \phi_{ij}(|\,\mathbf{x}^i-\mathbf{x}^j\,|) + \sum_{i\in\mathscr{L}} F_i(\rho_i),\end{aligned} \tag{2.1}$$

where

$$\rho_i = \sum_{\substack{j\in\mathcal{L}\\ j\neq i}} \psi_{ij}(|\,\mathbf{x}^i-\mathbf{x}^j\,|) \tag{2.2}$$

and $\phi_{ij}$, $F_i$, and $\psi_{ij}$ are real-valued functions. Assuming that there is a discrete field of body forces $\{\mathbf{F}^i\}_{i\in\mathscr{L}}$ acting on the defective lattice, a necessary condition for the current configuration $\{\mathbf{x}^i\}_{i\in\mathscr{L}} \subset \mathbb{R}^3$ to be in equilibrium is

$$-\frac{\partial\mathscr{E}}{\partial\mathbf{x}^i} + \mathbf{F}^i = \mathbf{0} \quad \forall i \in \mathscr{L}. \tag{2.3}$$

These discrete governing equations are highly nonlinear, in general. In order to be able to obtain semi-analytical solutions, we first linearize the governing equations with respect to a reference configuration $\mathscr{B}_0 = \{\mathbf{x}_0^i\}_{i\in\mathscr{L}}$. Note that this is the discrete analogue of linearizing the equations of nonlinear elasticity about a given motion [70,99]. One should also note that in molecular mechanics, there is no well-defined notion of reference configuration and all the existing interatomic potentials are defined in the current configuration (see [100] for a similar discussion). This is in contrast to elasticity where one always assumes a well-defined reference configuration, which may be thought of as a natural configuration of the material. However, in general, reference configuration could be any embedding of the material body in the physical space. Here, for us, reference configuration is some configuration of atoms that is not necessarily a local minimum of the total energy. We leave the reference configuration unspecified and will choose different reference configurations for different defects. At this point it would be enough to know that we usually choose the reference configuration to be a nominal defect configuration [97,98].

Taylor expansion of the governing equations for atom $i$, Eq. (2.3), about a reference configuration $\mathscr{B}_0 = \{\mathbf{x}_0^i\}_{i\in\mathscr{L}}$ reads

$$\begin{aligned}-\frac{\partial\mathscr{E}}{\partial\mathbf{x}^i} + \mathbf{F}^i = &-\frac{\partial\mathscr{E}}{\partial\mathbf{x}^i}(\mathscr{B}_0) - \frac{\partial^2\mathscr{E}}{\partial\mathbf{x}^i\partial\mathbf{x}^i}(\mathscr{B}_0)\cdot(\mathbf{x}^i-\mathbf{x}_0^i)\\ &- \sum_{\substack{j\in\mathcal{L}\\ j\neq i}} \frac{\partial^2\mathscr{E}}{\partial\mathbf{x}^j\partial\mathbf{x}^i}(\mathscr{B}_0)\cdot(\mathbf{x}^j-\mathbf{x}_0^j) - \ldots + \mathbf{F}^i = \mathbf{0}.\end{aligned} \tag{2.4}$$

Ignoring terms that are quadratic and higher in $\{\mathbf{x}^i - \mathbf{x}_0^i\}$, we obtain

$$\begin{aligned}&\frac{\partial^2\mathscr{E}}{\partial\mathbf{x}^i\partial\mathbf{x}^i}(\mathscr{B}_0)\cdot(\mathbf{x}^i-\mathbf{x}_0^i) + \sum_{\substack{j\in\mathcal{L}\\ j\neq i}} \frac{\partial^2\mathscr{E}}{\partial\mathbf{x}^j\partial\mathbf{x}^i}(\mathscr{B}_0)\cdot(\mathbf{x}^j-\mathbf{x}_0^j)\\ &= -\frac{\partial\mathscr{E}}{\partial\mathbf{x}^i}(\mathscr{B}_0) + \mathbf{F}^i \quad \forall i \in \mathscr{L}.\end{aligned} \tag{2.5}$$

Here $\left\{-\frac{\partial\mathscr{E}}{\partial\mathbf{x}^i}(\mathscr{B}_0)\right\}_{i\in\mathscr{L}}$ is the discrete field of *unbalanced forces*. Note that $\mathbf{f}_i^{\text{pair}} = -\frac{\partial\mathscr{E}^{\text{pair}}}{\partial\mathbf{x}^i}$, and $\mathbf{f}_i^{\text{cohesive}} = -\frac{\partial\mathscr{E}^{\text{cohesive}}}{\partial\mathbf{x}^i}$ are translation-invariant functions and thus one has the following relations for stiffness submatrices for pairwise and many-body interactions.

$$\frac{\partial^2\mathscr{E}^{\text{pair}}}{\partial\mathbf{x}^i\partial\mathbf{x}^i} = -\sum_{\substack{j\in\mathcal{L}\\ j\neq i}} \frac{\partial^2\mathscr{E}^{\text{pair}}}{\partial\mathbf{x}^j\partial\mathbf{x}^i}, \frac{\partial^2\mathscr{E}^{\text{cohesive}}}{\partial\mathbf{x}^i\partial\mathbf{x}^i} = -\sum_{\substack{j\in\mathcal{L}\\ j\neq i}} \frac{\partial^2\mathscr{E}^{\text{cohesive}}}{\partial\mathbf{x}^j\partial\mathbf{x}^i}, \tag{2.6}$$

i.e.,

$$\mathbf{K}_{ii}^{\text{pair}} = -\sum_{\substack{j\in\mathcal{L}\\ j\neq i}} \mathbf{K}_{ij}^{\text{pair}}, \mathbf{K}_{ii}^{\text{cohesive}} = -\sum_{\substack{j\in\mathcal{L}\\ j\neq i}} \mathbf{K}_{ij}^{\text{cohesive}}. \tag{2.7}$$

[3] Here by a "semi-analytic" method we mean a method that can obtain a fully nonlinear solution for an anharmonic lattice defect iteratively using exact harmonic solutions in each iteration.

[4] We should emphasize that the present formulation can be applied to long-range interactions as well. See Yavari et al. [98] for some relevant discussions.

The total substiffness matrix is now written as

$$\mathbf{K}_{ij} = \mathbf{K}_{ij}^{\text{pair}} + \mathbf{K}_{ij}^{\text{cohesive}}. \tag{2.8}$$

In many defective crystals one can simplify the calculations by exploiting partial symmetries. A defect, by definition, is anything that breaks the translation-invariance symmetry of the crystal. However, it may happen that a given defect does not affect the translation invariance of the crystal in one or two directions. With this idea, one can classify defective crystals into three groups: (i) defective crystals with 1-D symmetry reduction, (ii) with 2-D symmetry reduction and (iii) with no symmetry reduction [97]. Examples of (i), (ii) and (iii) are free surfaces, dislocations, and point defects, respectively. By convention, a perfect crystal is a defective crystal with 0-D symmetry reduction, i.e., it can be reduced to a unit cell.

Assume that the defective crystal $\mathscr{L}$ has a 1-D symmetry reduction, i.e., it can be partitioned into two-dimensional equivalence classes as

$$\mathscr{L} = \bigsqcup_{\alpha\in\mathbb{Z}} \bigsqcup_{I=1}^{N} \mathscr{L}_{I\alpha}, \tag{2.9}$$

where $\mathscr{L}_{I\alpha}$ is the equivalence class of all the atoms of type $I$ and index $\alpha$ with respect to the defect. Here we assume that $\mathscr{L}$ is a multilattice of $N$ simple lattices. For example, each equivalence class is a set of atoms lying on a plane parallel to the free surface. Fig. 1 schematically shows the idea of symmetry reduction for the case of $N = 3$. Each line represents an equivalence class, which can be a plane of atoms, a spherical shell of atoms, etc.

Using this partitioning (2.9) one can write

$$\sum_{\substack{j\in\mathscr{L}\\ j\neq i}} \frac{\partial^2 \mathscr{E}}{\partial \mathbf{x}^j \partial \mathbf{x}^i}(\mathscr{B}_0)\cdot(\mathbf{x}^j - \mathbf{x}_0^j) = \sum_{\alpha\in\mathbb{Z}}{}' \sum_{I=1}^{N} \sum_{j\in\mathscr{L}_{I\alpha}} \frac{\partial^2 \mathscr{E}}{\partial \mathbf{x}^j \partial \mathbf{x}^i}(\mathscr{B}_0)\cdot(\mathbf{x}^{I\alpha} - \mathbf{x}_0^{I\alpha}), \tag{2.10}$$

where the prime in the first sum in the right-hand side means that the term $\alpha = 0$, $I = i$ is omitted. The linearized discrete governing equations can be written as

$$\sum_{\alpha\in\mathbb{Z}}{}' \sum_{I=1}^{N} \mathbf{K}_{iI\alpha}\mathbf{u}^{I\alpha} + \left(-\sum_{\alpha\in\mathbb{Z}}{}' \sum_{I=1}^{N} \mathbf{K}_{iI\alpha}\right)\mathbf{u}^i = \mathbf{f}_i, \tag{2.11}$$

where

$$\begin{aligned} \mathbf{K}_{iI\alpha} &= \sum_{j\in\mathscr{L}_{I\alpha}} \frac{\partial^2 \mathscr{E}}{\partial \mathbf{x}^j \partial \mathbf{x}^i}(\mathscr{B}_0),\\ \mathbf{f}_i &= -\frac{\partial \mathscr{E}}{\partial \mathbf{x}^i}(\mathscr{B}_0) + \mathbf{F}_i,\\ \mathbf{u}^{I\alpha} &= \mathbf{x}^{I\alpha} - \mathbf{x}_0^{I\alpha} = \mathbf{x}^j - \mathbf{x}_0^j \quad \forall j \in \mathscr{L}_{I\alpha}. \end{aligned} \tag{2.12}$$

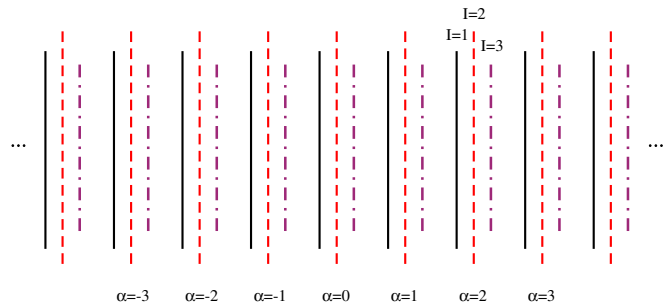


**Fig. 1.** Schematic partitioning of a defective multi-lattice with a 1-D symmetry reduction into equivalence classes for the case of $N = 3$.

Unit cell displacement vectors are defined as

$$\mathbf{U}_m = \begin{pmatrix} \mathbf{u}_m^1 \\ \vdots \\ \mathbf{u}_m^N \end{pmatrix} \in \mathbb{R}^{3N}. \tag{2.13}$$

Now the governing equations in terms of unit cell displacements are written as

$$\sum_{\alpha\in\mathbb{Z}} \mathbf{A}_\alpha(m)\mathbf{U}_{m+\alpha} = \mathbf{F}_m \quad m \in \mathbb{Z}, \tag{2.14}$$

where

$$\mathbf{A}_\alpha(m) \in \mathbb{R}^{3N\times 3N}, \mathbf{U}_\alpha, \mathbf{F}_m \in \mathbb{R}^{3N}. \tag{2.15}$$

This is a linear vector-valued ordinary difference equation with variable coefficient matrices. The unit cell force vectors and the unit cell stiffness matrices are defined as

$$\mathbf{F}_m = \begin{pmatrix} \mathbf{F}_{1m} \\ \vdots \\ \mathbf{F}_{Nm} \end{pmatrix}, \quad \mathbf{A}_\alpha(m) = \begin{pmatrix} \mathbf{K}_{11\alpha} & \mathbf{K}_{12\alpha} & \cdots & \mathbf{K}_{1N\alpha} \\ \mathbf{K}_{21\alpha} & \mathbf{K}_{22\alpha} & \cdots & \mathbf{K}_{2N\alpha} \\ \vdots & \vdots & \cdots & \vdots \\ \mathbf{K}_{N1\alpha} & \mathbf{K}_{N2\alpha} & \cdots & \mathbf{K}_{NN\alpha} \end{pmatrix} \quad \forall m \in \mathbb{Z}. \tag{2.16}$$

Note that, in general, $A_\alpha$ need not be symmetric [97]. Note also that $\mathbf{A}_\alpha$ explicitly depends on $m$ only close to the defect.

## 3. Semi-analytic analysis of single defects in crystals

Our goal in this paper is to develop a general framework in which one can study the structures and energetics of different types of defects in crystals with possibly many-body interactions. In order to demonstrate the capability of our anharmonic lattice statics formulation in serving as such a framework, we solve several defect problems in the sequel.

Another use of our formulation is its ability in serving as a tool for comparing different interatomic potentials. An interatomic potential can be thought of as a "discrete constitutive equation" and hence different interatomic potentials would, in general, predict different structures and energetics for a given defect in a material system. This interesting and important problem of qualitatively and quantitatively comparing different interatomic potentials has been overlooked in the literature of computational physics. As we will see in the sequel, our general framework is capable of making quantitative and qualitative comparisons of different interatomic potentials for a given crystalline material. We will also see that, in general, two different interatomic potentials predict different structures and energies for the same defect in a given crystalline solid.

We will work on the following four examples:

- Point defect in fcc Cu.
- (001) surface defect in fcc Cu.
- $\Sigma(5)$ symmetric twin boundary in fcc Cu.
- $\Sigma(5)$ symmetric twin boundaries in the shape memory alloy NiAl.

The first three examples, although have different partial symmetries, can all be reduced to 1-D defect problems and the last problem is an example of defects in multi-lattices. In the following, the interatomic potentials used in our numerical examples are briefly explained.

### 3.1. Potentials used in the examples

It is well known that two-body interatomic potentials such as the classical Lennard-Jones type potentials have serious limitations

and cannot represent interatomic interactions in most real crystals; failure of the Cauchy relations is an example [83,12].

However, by using many-body potentials such as those proposed by Daw and Baskes [21], Finnis and Sinclair [29] and Ercolessi et al. [25], these restrictions can be overcome. Although these potentials were proposed with different physical motivations, the static crystal energy in all of them can be written generically as

$$\mathscr{E}^{\text{stat}} = \frac{1}{2}\sum_{\substack{i,j\in\mathcal{L}\\ j\neq i}} \phi_{ij}(r_{ij}) + \sum_{i\in\mathscr{L}} F_i(\rho_i), \tag{3.1}$$

where $F_i(\rho_i)$ represents the energy of "embedding" atom $i$ in the electric density $\rho_i$ created by all other atoms in the crystal. The core–core repulsion between atoms $i$ and $j$ is represented by $\phi_{ij}$, which depends on the type of atoms $i$ and $j$ and the distance between them. The electron density $\rho_i$ is the sum of the electron density contributions of all other atoms at the nucleus of atom $i$ and is written as

$$\rho_i = \sum_{\substack{j\in\mathcal{L}\\ j\neq i}} \psi_{ij}(r_{ij}), \tag{3.2}$$

where $\psi_{ij}(r_{ij})$ is the electron density contribution from atom $j$ at a distance $r_{ij}$ from atom $i$.

The following potentials are used in our calculations.

*Sutton–Chen potential (SC potential).* This is a potential of the EAM type developed by Sutton and Chen [86] (see also [59]), where the following functions represent the pairwise and many-body interactions in Eq. (3.1), respectively

$$\phi_{ij}(r_{ij}) = \frac{\epsilon a^n}{r_{ij}^n}, \quad F_i(\rho_i) = -c\epsilon\sqrt{\rho_i}, \quad \psi_{ij}(r_{ij}) = a^m r_{ij}^{-m}. \tag{3.3}$$

For copper we use the following numerical values [59,78]

$$n = 9,\ m = 6,\ \epsilon = 1.2386\times 10^{-2}\ \text{eV},\ c = 39.755,\ a = 3.616\ \text{Å}. \tag{3.4}$$

*Quantum Sutton–Chen potential (QSC potential).* In this potential [86,59], the same functions (3.3) are used for the pairwise and many-body interactions but for copper the following potential parameters [59,78] are used.

$$n = 10,\ m = 5,\ \epsilon = 5.7921\times 10^{-3}\ \text{eV},\ c = 84.843,\ a = 3.593\ \text{Å}. \tag{3.5}$$

*Barrera et al. potential (B potential).* As the third potential of the EAM type, we chose the potential developed by Barrera et al. [6]. For the electronic densities, the following simple exponential function is used

$$\psi_{ij}(r_{ij}) = A\exp\left(\frac{-r_{ij}}{\sigma^e}\right), \tag{3.6}$$

which is associated with the following embedding energy

$$F_j = -C\sqrt{\rho_j}. \tag{3.7}$$

The repulsive or the pairwise potential is of a simple exponential form

$$\phi_{ij}(r_{ij}) = B\exp\left(\frac{-r_{ij}}{\sigma^r}\right). \tag{3.8}$$

For fcc copper we have the following numerical values [6] for this potential

$$B = 7076.56\ \text{eV},\ \sigma^r = 0.241535\ \text{Å}, A = 188.542,\\ \sigma^e = 0.536562\ \text{Å}, C = 1\ \text{eV},\ a = 3.6149\ \text{Å}. \tag{3.9}$$

*NiAl EAM potential.* We use the second-moment interatomic potential for Al, Ni and Ni–Al alloy of EAM type developed by Papanicolaou et al. [77]. In this potential, the electron density function has the following exponential form:

$$\psi_{ij}(r_{ij}) = \xi_{\alpha\beta}^2 \exp\left[-2q_{\alpha\beta}\left(\frac{r_{ij}}{r_0^{\alpha\beta}} - 1\right)\right] \tag{3.10}$$

associated with the following embedding energy

$$F_j = -C\sqrt{\rho_j}. \tag{3.11}$$

The repulsive pairwise potential is of the form

$$\phi_{ij}(r_{ij}) = A_{\alpha\beta}\exp\left[-p_{\alpha\beta}\left(\frac{r_{ij}}{r_0^{\alpha\beta}} - 1\right)\right]. \tag{3.12}$$

The potential parameters for Al–Al, Ni–Ni, and Ni–Al interactions are:

$$\begin{aligned}
&\text{Al}-\text{Al}: \xi_{\alpha\beta} = 0.9564\ \text{eV},\ A_{\alpha\beta} = 0.05504\ \text{eV},\ q_{\alpha\beta} = 1.5126,\\
&\qquad p_{\alpha\beta} = 10.9011,\ r_0^{\alpha\beta} = 2.8310\ \text{Å},\\
&\text{Ni}-\text{Ni}: \xi_{\alpha\beta} = 1.4175\ \text{eV},\ A_{\alpha\beta} = 0.07415\ \text{eV},\ q_{\alpha\beta} = 2.2448,\\
&\qquad p_{\alpha\beta} = 13.8297,\ r_0^{\alpha\beta} = 2.4307\ \text{Å},\\
&\text{Ni}-\text{Al}: \xi_{\alpha\beta} = 1.4677\ \text{eV},\ A_{\alpha\beta} = 0.09493\ \text{eV},\ q_{\alpha\beta} = 3.8507,\\
&\qquad p_{\alpha\beta} = 10.9486,\ r_0^{\alpha\beta} = 2.7424\ \text{Å}.
\end{aligned} \tag{3.13}$$

We choose a force tolerance of $f = 0.05$ eV/Å for the calculations of the distorted atomic configurations. However, we will numerically study the effect of the force tolerance on the structure and energy of point defects.

### 3.2. Example 1: a single point defect in fcc copper

Distortion of a crystal lattice due to point defects, e.g., substitutional or interstitial atoms or vacant lattice sites has been a problem of interest for a long time. The very first attempt to model this problem was to treat the point defect as a center of dilatation in an infinite isotropic elastic medium [69,26]. In early 1950s the interaction of the boundaries and point defects was considered by Eshelby, and Johnson [26,27,50]. Kanzaki [55,56] proposed a method for the calculation of distortions around a point defect in an fcc crystal without any reference to continuum solutions. In this method, a system of equilibrium equations was derived using an appropriate pair potential, and then with application of the discrete Fourier transform (DFT) method the equations were decoupled in the reciprocal space. The proposed method and some of its variations were later on called *method of lattice statics* and were used by several other authors for solving similar point defect problems. The reader is referred to [30,31,33,32,58,34,97,98], and references therein for more details.

Another class of methods consider the defective lattice discrete close to the defect and continuum far from the defect [42,91,8,53,51,54,50,52]. Hall [42] was among the first who explicitly exploited the radial symmetry of point defects in fcc lattices in his numerical calculations. In his work, for pure metals, atoms of equal distances from the defect, all have radial displacements and forces of equal magnitudes [42,51]. Some other authors obtained the relaxed configuration in an iterative process by relaxing the shells of atoms successively using the force constants until convergence was achieved [44,39,40,53,51,54,50,52].

An alternative approach to obtain the fully nonlinear solutions of point defect problems was proposed by Flocken [35], where the first and second shells were relaxed successively, while the rest of atoms were relaxed using the standard method of lattice statics. In this method, the forces were calculated exactly in contrast to the standard lattice statics method. Another method for solving point

defect problems is the method of lattice Green's function (see [23,22,90] and references therein). It can be seen that point defects in crystals have been analyzed more or less using heuristic approaches and not within a general framework. In the following, we study a single point defect in an infinite simple lattice and show how its governing equations can be reduced using symmetry conditions.

*Symmetry reduction in a point defect problem.* It turns out that in the case of a single point defect in fcc Cu displacements with respect to the reference configuration are radial, i.e. those atoms that are equidistant from the vacant site have the same unbalanced forces and displacements [42]. This is also the case in the continuum approach for the solutions of point defect problems, where the point defect is considered to be the center of dilatation in the elastic medium and all the atoms are constrained to have $O(1/r^2)$ displacements, where $r$ is distance from the defect. In our numerical calculations, the material body is partitioned into two regions: Region I contains atoms in the vicinity of the defect and Region II contains the atoms away from the defect. The atoms in Region I are relaxed according to their individual equivalence classes. Region II atoms are relaxed with displacements proportional to $1/r^2$.

The radial symmetry of the point defect problem enables one to reduce the discrete governing equations to an ordinary difference equation on $\mathbb{N}$. Each equivalence class is a set of atoms lying on a spherical shell and this partitions the lattice $\mathscr{L}$ as

$$\mathscr{L} = \bigsqcup_{n=1}^{\infty} \mathscr{L}_n. \tag{3.14}$$

For atoms in the equivalence class $\mathscr{L}_n$ we know that

$$\mathbf{u}^i = u_n \hat{\mathbf{r}}^i \quad \forall i \in \mathscr{L}_n, \tag{3.15}$$

where $\hat{\mathbf{r}}^i = \mathbf{x}_0^i / |\mathbf{x}_0^i|$. In the equilibrium configuration $\mathscr{B} = \{\mathbf{x}^i\}_{i\in\mathscr{L}}$ one has

$$\frac{\partial \mathscr{E}}{\partial \mathbf{x}^i} = \mathbf{0} \quad \forall i \in \mathscr{L}. \tag{3.16}$$

Because all atoms in an equivalence class have the same magnitude of force this is equivalent to

$$\frac{\partial \mathscr{E}}{\partial \mathbf{x}^I} = \mathbf{0} \quad \forall I \in \mathbb{N}, \tag{3.17}$$

where $I$ is a representative of the equivalence class $\mathscr{L}_I$. Linearization of equilibrium equations about a reference configuration $\mathscr{B}_0 = \{\mathbf{x}_0^i\}_{i\in\mathscr{L}}$ yields

$$\sum_{n=1}^{\infty} \sum_{j\in\mathscr{L}_n} \frac{\partial^2 \mathscr{E}}{\partial \mathbf{x}^j \partial \mathbf{x}^I}(\mathscr{B}_0) \cdot \mathbf{u}^j = \mathbf{f}_I \quad \forall I \in \mathbb{N}. \tag{3.18}$$

Or

$$\sum_{n=1}^{\infty} \mathbf{k}_{In} \cdot u_n \hat{\mathbf{r}}^I = \mathbf{f}_I \quad \forall I \in \mathbb{N}, \tag{3.19}$$

where $\mathbf{f}_I$ is the unbalanced force on the representative of the equivalence class $\mathscr{L}_I$ and

$$\mathbf{k}_{In} = \sum_{j\in\mathscr{L}_n} \frac{\partial^2 \mathscr{E}}{\partial \mathbf{x}^j \partial \mathbf{x}^I}(\mathscr{B}_0) \hat{\mathbf{r}}^j. \tag{3.20}$$

*Relaxation method.* The anharmonic solution of the point defect problem is obtained using the following algorithm. First, we construct a reference configuration by creating a vacant site preferably at the center of a finite but large perfect crystal (material body). Then, we choose a spherical volume of an appropriate size contained in the material body (smaller in size than the material body) centered at the vacant site and call it the relaxation volume. Atoms in this volume are classified according to their distances from the vacant site, and therefore atoms of the same class lie on the same shell centered at the vacant site. The relaxation volume contains a collection of shells, where each shell represents an equivalent class of atoms. The atoms inside the relaxation volume are relaxed through an iterative process, where in each iteration the force and stiffness for an individual shell is calculated exactly and then all the atoms on that individual shell are displaced accordingly.

In the relaxation process, when the absolute values of all the unbalanced forces in the configuration are less than a certain small positive number (force tolerance), the iterative process is stopped. This force tolerance is usually chosen in the interval 0.01–0.05 eV/Å. The choice of the force tolerance strongly affects the relaxed configuration and also the energetics. Therefore, for any choice of the force tolerance a sensitivity test has to be conducted to accurately identify the minimum necessary radius of the region around the point defect with atomic interactions (the relaxation volume size) so that the displacements of the atoms in the volume exterior to the relaxation volume is invariant under choices of relaxation volumes with radii larger than the minimum radius determined.

In particular, for smaller values of the force tolerance larger relaxation volumes have to be chosen. Therefore, the relaxed configuration strongly depends on the potential and also on the choice of the force tolerance, in general. A measure of the importance of the relaxation volume size is $\Delta E_0/W_0$, where $\Delta E_0$ is the relaxation energy and $W_0$ is the energy of formation of a vacancy without distortion under zero pressure. Increasing the volume size, the ratio $\Delta E_0/W_0$ increases until a plateau is reached. Any size larger than this threshold is appropriate. As an example, it is seen in [42] that $\Delta E_0$ varies from 1.78% to about 12% of $W_0$ as the reduced volume decreases from 1.0 to 0.4, where the reduced volume corresponds to the reduced radius, which is the radius normalized by the first nearest neighbor distance.

In the case of a vacancy, in some previous works (for example, [39]) where the interatomic interactions were pairwise, only the nearest and next nearest neighbors from the vacancy needed to be considered in energy calculations. However, this is not necessarily the case when many-body interatomic interactions are present; this is geometry and material dependent and given an interatomic potential it should be numerically studied.

*Numerical results.* Girifalco and Weizer [40] reported the reduced displacement values (the displacement normalized by the first nearest neighbor distance) for the first and second nearest neighbors from the vacant site and the energies of relaxation were mentioned to be −2.24%, 0.4% and 0.56 eV, respectively (negative sign means displacement towards the vacant site or contraction of the shell). We choose this work as a reference for comparison. We calculated the distortion around a vacancy with two force tolerances of 0.05 eV/Å and 0.02 eV/Å, using all the three previously mentioned potentials to demonstrate the sensitivity of the relaxed configuration and its energy to the choice of force tolerance and potential.

Using SC potential and the choice of $f = 0.05$ eV/Å we obtained −0.7%, and 0.0% for the reduced displacements of the first and second nearest neighbors, respectively, and 0.486 eV for the relaxation energy, while the choice of $f = 0.02$ eV/Å resulted in the reduced displacements of −1.4%, and −0.05% for the first and second nearest neighbors, respectively, and 1.395 eV for the relaxation energy. It is also noteworthy to mention that the first choice of the force tolerance resulted in distortion of only the first nearest neighbor atoms from the vacant site with respect to the reference configuration while the second choice resulted in the distortion of atoms in the first four nearest shells from the vacant site and a configuration with lower energy.

The QSC potential with the choice of $f = 0.05$ eV/Å resulted in −0.87%, and 0.0% reduced displacements of the first and second nearest neighbors, respectively, and 0.679 eV for the relaxation

energy, while the choice of 0.02 eV/Å for the force tolerance resulted in −1.8%, and −0.03% for the first and second nearest neighbors, respectively, and 1.906 eV for the relaxation energy. Using QSC Potential, and the choice of $f = 0.05$ eV/Å a relaxed configuration with distortions in only the first nearest neighbor atoms from the vacant site was obtained, while the choice of $f = 0.02$ eV/Å resulted in a relaxed configuration with distortions in atoms in the first 11 shells.

We also calculated the reduced displacements of the first and second nearest neighbors of magnitudes −1.9%, and 0.0% and the relaxation energy of 1.77 eV for $f = 0.05$ eV/Å and −2.5%, and −0.4% and the relaxation energy of 1.69 eV for $f = 0.02$ eV/Å using the B potential. Using B potential, the first choice of force tolerance resulted in the distortion of atoms in the first 11 shells from the vacant site while for the second force tolerance choice it resulted in the distortion of the first 80 shells. It is apparent that our results are reasonably close to the results of Girifalco and Weizer [40] although in that work only pairwise interactions were considered. The sensitivity of the calculated relaxed configuration and in particular the size of the distorted volume and relaxation energy on the choice of the force tolerance and potential is clearly seen in these numerical calculations.

Now, it is easy to compare the results from the three different potentials. As it is seen in Figs. 2 and 3, in the case of 0.05 eV/Å force tolerance, the results from SC and QSC potentials are very close to each other and only the nearest neighbor atoms from the vacant site are distorted, while using the B potential results in distortion of atoms in the first 11 shells closest to the vacant site. This is also the case with the 0.02 eV/Å choice of force tolerance, where SC and QSC predicted distortion of atoms in the first 4 and 11 shells, respectively, while for the B potential the distortions occur in the first 80 shells. This means that the distortion volume strongly depends on the choice of the potential and for some potentials (B potential), the distortion volume is much larger than other choices of potentials (SC and QSC potentials).

### 3.3. Example 2: (001) surface defect in fcc copper

Structures, energetics and in general study of surface defects is of fundamental importance, as any real crystal is finite and has free surfaces. Theoretical calculations of the effects of surface forces on defects within a crystal as well as formation and migration energies of defects on the crystal surfaces have been of interest for quite sometime.

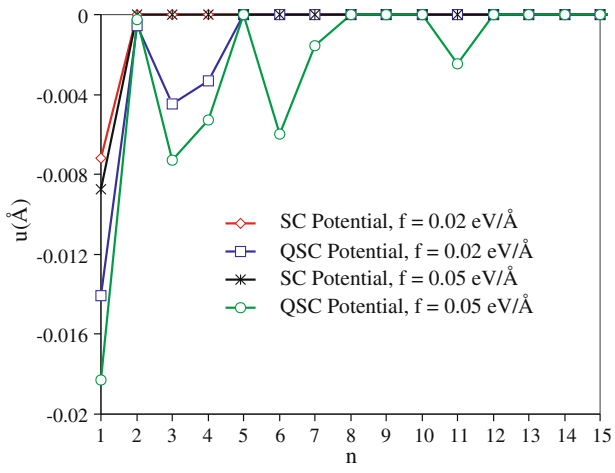


**Fig. 2.** Anharmonic displacements of atomic shells with respect to the reference configuration.

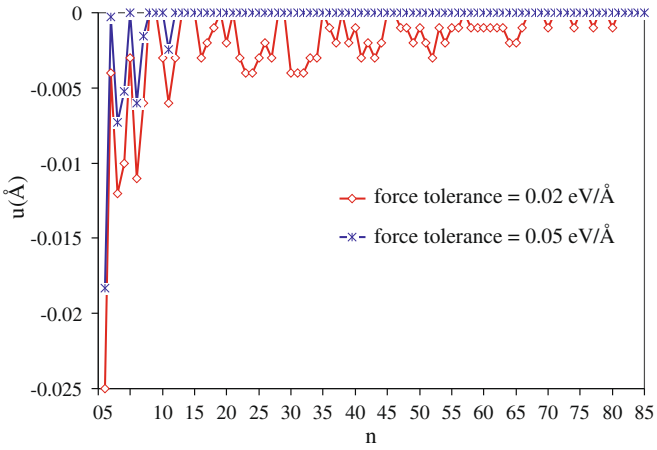


**Fig. 3.** Anharmonic displacements of atomic shells with respect to the reference configuration for the force tolerances of 0.02 eV/Å and 0.05 eV/Å using the B potential.

In the so-called direct space method, one starts with a perfect lattice with a boundary surface of proper orientation. Then the surface is relaxed by an iterative process until the net force on each atom is less than a force tolerance. This method was used by Wynblatt and Gjostein in calculation of migration and formation energies for surface defects in copper [95] and tungsten [94], by Bonneton and Drechsle [11] in their calculations of atomic relaxation near a (1 1 2) surface in W, Mo, and Ta, and by Jackson [48] in calculation of the relaxations of atoms in a number of fcc and bcc metals (see also [61]). The advantage of using the direct-space method is that forces can be calculated explicitly using a reliable potential. However, the number and complexity of the governing equations rapidly increases as the size of the model increases.

Another method is the Green's function method where one considers a supercell with $N$ atoms that contains the defect and then periodically repeats it in space. The resulting $3N \times 3N$ set of equilibrium equations in each supercell is then solved using DFT. Feuchtwa [28] developed a comprehensive formalism to determine atomic displacements near surfaces in fcc lattices using the Green's function method. Corciove et al. [17] in an attempt to determine the general characteristics of atomic displacements near surfaces in fcc lattices employed the Green's function method, where all the anharmonic effects are neglected and the static displacements are directed along the normal to the surface in order to satisfy the invariance requirements. Detailed calculations were done for a finite slab in the nearest neighbor approximation and the periodic boundary conditions were applied.

An advantage of using Green's function method is that the supercells can be made very large and thus the Fourier sums can be converted into integrals that would lead to some asymptotic solutions for defects. This idea was developed by Hardy and Flocken [45], Flocken [34], and Boyer and Hardy [14], and later used by Flocken [36] for surface defect problems. One disadvantage of this method is that it can be used only for harmonic lattices. Tewary [88] and Tewary and Bullough [89] developed a method to carry out the entire calculation in the reciprocal space without the direct-space potential being known explicitly. For more examples of relevant analyses of the surface defect problems see [66,46,57,93,43,41,47,101–103] and references therein.

Another method that employs both hypotheses of Green's function method and the direct-space method and is able to capture anharmonic effects is called the modified lattice statics method [37]. In the modified lattice statics method, for free surfaces, the first few layers (usually the first two layers) are successively

relaxed using the direct-space method and the remainder of the lattice is relaxed iteratively using the Green's function method.

The most common result in all the above-mentioned works was the oscillatory behavior of the interlayer spacings close to a free surface in the relaxed configuration. Starting from an undistorted configuration of a free surface with perfect lattice spacings, the results confirmed a decrease in the interlayer spacing between the first and second layers (assuming that the first layer is the boundary) and an increase in the interlayer spacing between the second and the third layers in the relaxed configuration [7,66,57,93,16]. Babŭska and his coworkers [4] were among the first who studied simple defects in harmonic lattices and proposed a general method of solution of the governing equations using the method of discrete Fourier transform [5].

*Discrete boundary-value problem of a free surface.* Before discussing the boundary-value problem of an arbitrary free surface, let us first look at a simple half chain of atoms with first and second nearest neighbor interactions with respective spring constants $k_1$ and $k_2$ (see Fig. 4). In a real free surface, these force constants can be obtained by exploiting symmetry conditions and linearizing the governing equations with respect to a reference configuration. We assume that unbalanced forces are nonzero only for the first two layers and denote them by $f_0$ and $f_1$. The bulk equilibrium equation is written as (see also [15] for similar discussions)

$$n \geqslant 2 : k_1(x_{n+1} - 2x_n + x_{n-1}) + k_2(x_{n+2} - 2x_n + x_{n-2}) = 0. \tag{3.21}$$

The boundary equations are

$$n = 0 : k_1(x_1 - x_0) + k_2(x_2 - x_0) = f_0, \tag{3.22}$$
$$n = 1 : k_1(x_2 - 2x_1 + x_0) + k_2(x_3 - x_1) = f_1. \tag{3.23}$$

Assuming that $x_n = c\lambda^n$ is a solution one obtains the following characteristic equation [1,24,65]

$$k_2 + k_1\lambda - 2(k_2 + k_1)\lambda^2 + k_1\lambda^3 + k_2\lambda^4 = 0. \tag{3.24}$$

The above fourth order polynomial has the following four roots

$$\lambda_1 = \frac{-k_1 - 2k_2 - \sqrt{k_1(k_1 + 4k_2)}}{2k_2}, \quad \lambda_2 = \lambda_3 = 1,$$
$$\lambda_4 = \frac{-k_1 - 2k_2 + \sqrt{k_1(k_1 + 4k_2)}}{2k_2} \tag{3.25}$$

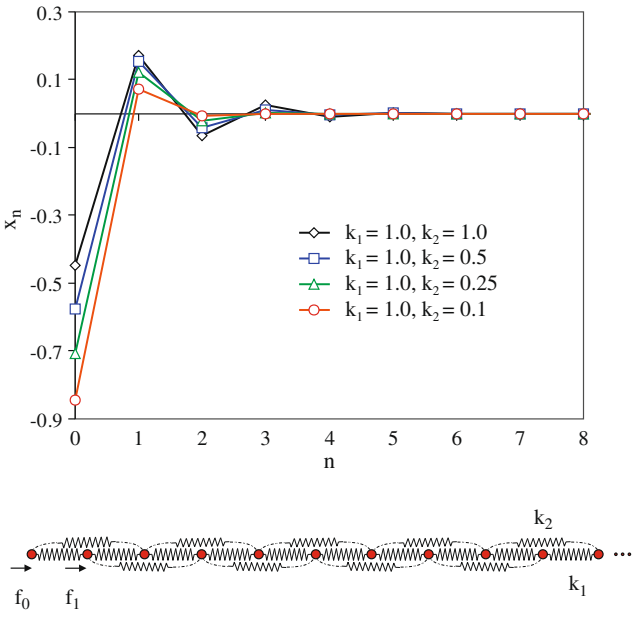


**Fig. 4.** Harmonic displacements for a half-chain model of a free surface.

and the general solution is now written as

$$x_n = c_1\lambda_1^n + c_2 n + c_3 + c_4\lambda_4^n \quad n \geqslant 0. \tag{3.26}$$

Note that $|\lambda_1| > 1$ and $|\lambda_4| < 1$. Let us first assume that displacements are bounded at infinity. Thus

$$x_n = c_3 + c_4\lambda_4^n \quad n \geqslant 0. \tag{3.27}$$

Boundary equations read

$$c_4[-(k_1 + k_2) + k_1\lambda_4 + k_2\lambda_4^2] = f_0, \tag{3.28}$$
$$c_4[k_1 - (2k_1 + k_2)\lambda_4 + k_1\lambda_4^2 + k_2\lambda_4^3] = f_1. \tag{3.29}$$

This means that $f_0$ and $f_1$ cannot be arbitrary and have to satisfy the following relation

$$\frac{f_0}{f_1} = \frac{-(k_1 + k_2) + k_1\lambda_4 + k_2\lambda_4^2}{k_1 - (2k_1 + k_2)\lambda_4 + k_1\lambda_4^2 + k_2\lambda_4^3} = -1, \tag{3.30}$$

i.e., the external forces must be self-equilibrated. Arbitrariness of $c_3$ is a consequence of translation invariance and we can choose $c_3 = 0$. Let us now assume the numerical values $k_1 = 1$, $f_0 = 1$ and calculate the harmonic displacements of the atomic layers in the vicinity of the surface defect for choices of $k_2 = 1$, $k_2 = 0.5$, $k_2 = 0.25$, and $k_2 = 0.1$. The harmonic displacements are shown in Fig. 4. Note that even this very simple model exhibits the oscillatory displacement behavior observed in real crystal surfaces and more interestingly, smaller values of $k_2/k_1$ result in larger displacements of the first layer but faster decay of displacements away from the free surface.

If the force system $\{f_0, f_1\}$ is not self-equilibrated, physically we expect a uniform expansion or compression in addition to the above localized displacements. This means that in (3.26) $c_2 \neq 0$. Note that

$$x_{n+1} - x_n = c_2 + c_4\lambda_4^n(\lambda_4 - 1) \quad n \geqslant 0. \tag{3.31}$$

This means that

$$|\, x_{n+1} - x_n \,| < \infty \text{ as } n \to \infty \tag{3.32}$$

i.e., the field of *discrete strains* is bounded at infinity. Imposing the boundary conditions (3.28) and (3.29), we obtain

$$c_2 = \frac{f_0 + f_1}{k_1 + 4k_2}, \quad c_4 = \frac{2(f_0 - f_1)k_2 - f_1 k_1}{(k_1 + 4k_2)\sqrt{k_1(k_1 + 4k_2)}}. \tag{3.33}$$

Note that the uniform expansion/compression term is nonzero only if the pressure $f_0 + f_1$ is nonzero (see [38] for a similar discussion). It is also seen that, in general, the displacement field is the superposition of a uniform expansion/compression and a localized surface displacement field.

A (100) free surface is an example of a defective lattice with a 1-D symmetry reduction. Therefore, the governing equations can be written for a chain of representative unit cells (atoms in the case of Cu simple lattice). A natural approach for solving this problem is to write the linearized governing equations for a half chain of atoms, i.e.

$$\sum_{\alpha=-m}^{m} \mathbf{A}_\alpha \mathbf{X}_{n+\alpha} = \mathbf{F}_n; \quad n \geqslant m + 1 \tag{3.34}$$

with $m$ boundary equations, where $m$ is the range of unit cell interactions, i.e., unit cell $n$ interacts with its first $m$ nearest-neighbor unit cells. One also needs to impose boundedness of displacements at infinity (or the weaker condition of boundedness of displacement differences) and should also fix the translation invariance of the defective lattice by fixing an atom. Thus, all one needs to have are stiffness matrices and unbalance forces $\{\mathbf{F}_n\}_{n\in\mathbb{N}}$. Given any interatomic potential, one can calculate forces close to the free surface and because the far field is the bulk configuration, forces would decay to zero away from the free surface. In summary, the discrete

boundary-value problem (DBVP) of a free surface has the following form

$$\sum_{\alpha=-m}^{m} \mathbf{A}_\alpha \mathbf{X}_{n+\alpha} = \mathbf{F}_n \quad n \geqslant m+1, \tag{3.35}$$

$$\sum_{\alpha=-m}^{m} \mathbf{A}_\alpha(n) \mathbf{X}_{n+\alpha} = \mathbf{F}_n \quad n = 0, 1, \ldots, m, \tag{3.36}$$

$$\lim_{n\to\infty} \|\mathbf{X}_{n+1} - \mathbf{X}_n\| < \infty. \tag{3.37}$$

To further investigate the state of forces near a surface defect we used a 2-D model of a complex lattice with a Lennard-Jones type potential [60]. The diatomic lattice has two stable atomic configurations which are hexagonal and complex square lattices. For this numerical study we choose the square complex lattice with two types of atoms A,B. The following are the LJ potential and the parameters chosen

$$\Phi_{\alpha\beta}(x_{\alpha\beta}) = 4\varepsilon_{\alpha\beta}\left[\left(\frac{\sigma_{\alpha\beta}}{x_{\alpha\beta}}\right)^{12} - \left(\frac{\sigma_{\alpha\beta}}{x_{\alpha\beta}}\right)^{6}\right],$$

$$\varepsilon_{AB} = \varepsilon_{BB} = \varepsilon_{AA} = 2.5 \times 10^{-10}\ \text{m}, \sigma_{AA} = \sigma_{BB} = \sqrt{2}\sigma_{AB} = 10 \times 10^{-19}\ \text{J},$$

where only the first and second nearest neighbor interactions are considered. The results of our force calculation confirms that the forces on a half lattice are not self-equilibrated and we obtained forces of magnitude $4.1377 \times 10^{-8}$ N for each atom on the surface and forces of magnitude $1.37923 \times 10^{-8}$ N on each atom on the second layer from the surface. This can be numerically checked for more complicated lattices and in all the numerical examples we have studied, forces near a free surfaces are not self-equilibrated. Let us consider a finite cubic part of a cubic lattice (Fig. 5 shows a planar projection). If this cube is large enough, forces would be nonzero only in the gray regions close to free surfaces. Because of symmetry forces on the face 1, for example, would cancel forces on face 2. Therefore, to analyze a free surface one can extend the cube to infinity in two directions and consider a slab. Again, forces would be nonzero only in the gray regions shown in the figure. It turns out that, in general, forces on one face are not self-equilibrated and that is why one should expect a uniform expansion/compression in addition to the localized surface displacements.

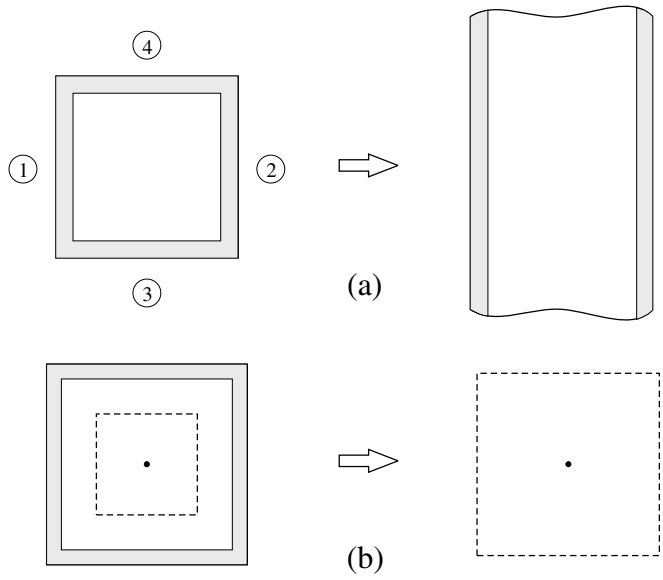


**Fig. 5.** (a) A finite crystal with free surfaces. One can study the structure of free surfaces by moving faces 3 and 4 to infinity and solving a slab problem. (b) A point defect in a finite crystal. Increasing the size of the crystal, one can assume that a single point defect is embedded in an infinite crystal.

Nevertheless, one can consider the atoms in the white region, far enough from the free surface and to a good approximation not distorted. Therefore, those atoms far from the free surface can be fixed to their perfect lattice positions (bulk lattice) and the atoms in the vicinity of the surface can be displaced to obtain the relaxed configuration and model a free surface as a semi-infinite lattice.

In the case of a point defect, for example, one can again consider a finite crystal centered at the defect (see Fig. 5b). For a large enough cube, one can find a smaller cube centered at the defect where the free surface effects are absent. Thus, in the limit, one can assume that there is a point defect in an infinite crystal.

*Simultaneous harmonic relaxation.* As we discussed earlier, to model a free surface one might either consider a slab of finite dimension (in this case a sensitivity test should be conducted to assure the correct choice of the slab size) or a semi-infinite lattice. Therefore, the first step would be to construct the material body as we did in the previous example. We construct the material body from a finite perfect crystal, where atoms are in their perfect crystal lattice sites. We also perform a sensitivity test to make sure that the size of the slab is chosen reasonably so that there are some atomic layers in the middle region of the slab not affected (with respect to the force tolerance) by the free surfaces and can be considered as bulk. We then use the classification method to classify the atoms in the material body according to their normal distances from the slab surfaces, so that the atoms of the same distance from the free surface belong to the same class and in the relaxation procedure they are displaced together. We relax the atoms in the material body using an iterative algorithm in which in each iteration force vectors and stiffness matrices of all the classes are calculated, then evaluate their corresponding displacements, and update the position of all the atoms in every class. In order to calculate the force vector and stiffness matrix of a class of atoms we pick an atom from that class as the class representative and calculate its force vector and stiffness matrix. We proceed with iterations until a desired force tolerance is achieved.

It should be mentioned that the choice of the force tolerance is crucial in the appropriate size of the slab (the sensitivity test would identify the right size of the slab depending on the choice of the force tolerance and the potential); if we choose a small force tolerance we most likely have to increase the size of the slab.

The following is our *simultaneous anharmonic lattice statics* algorithm:

Input data: Defective crystal geometry, interatomic potential, force tolerance, slab size $N$
- ▹Initialization
  - ▹Construct the reference configuration $\mathscr{B}_0$
  - ▹Calculate unbalanced forces $\mathbf{F}^0 = \mathbf{F}(\mathscr{B}_0)$
  - ▹Assemble substiffness matrices and construct $\mathbf{K}_0$
  - ▹Calculate displacements $\mathbf{U}^0 = \mathbf{K}_0^{-1}\mathbf{F}^0$
- ▹Do until convergence is achieved
  - ▹$\mathscr{B}_0^{k+1} = \mathscr{B}_0^k + \mathbf{U}^k$
  - ▹Update substiffness matrices and construct $\mathbf{K}_k$
  - ▹Calculate displacements $\mathbf{U}^{k+1} = \mathbf{K}_k^{-1}\mathbf{F}^k$
- ▹End Do
- ▹

*Numerical results.* We use all the three potentials to calculate the corresponding relaxed configurations. Note that some previous studies suggest the relaxation of the first 8 layers for the low index surfaces and the first 13 layers for the high index surfaces[5] [93]. We

[5] High index surfaces are those for which at least one of the Miller indices is a relatively large number.

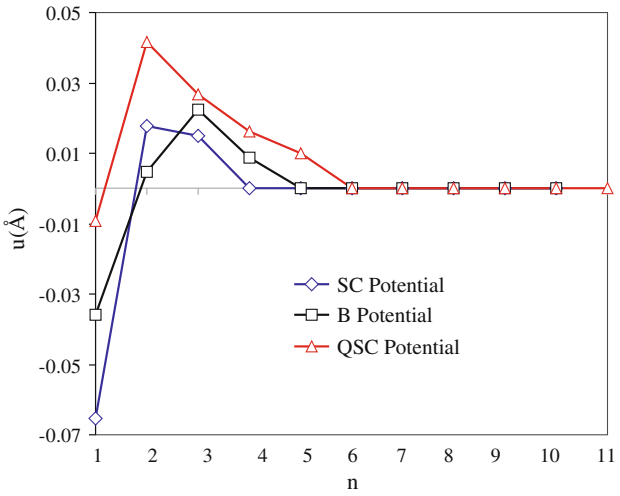


**Fig. 6.** Anharmonic displacements for a (001) free surface in fcc Cu with respect to the reference configuration.

observe that this rule of thumb works, at least for fcc Cu with the three given EAM potentials; surface structure is independent of slab thickness for slabs thicker that 21 layers (one layer in the middle and 10 layers on each side). However, this is problem dependent and should be studied carefully for a given material system.

Our results using all the three potentials confirm the contraction in the first interlayer spacing and expansion in the second interlayer spacing of (100) surface defect in fcc copper. For Cu (100) surface defect, experimental results [18,19,67,72] suggest a contraction ranging from −1.0% to −2.1% in the first and second layers, the modified EAM [93] gave −0.83% while the results of EAM [75] and effective-crystal theory [80] were −3.79% and −3.7%, respectively. Our calculations predict contraction of the first interlayer spacing of −3.6% using SC potential, −0.52% using QSC potential, and −1.98% for the B potential. The results from the B Potential is in very good agreement with the experimental data. The changes in the interlayer spacings of half of the slab is shown in Fig. 6. The relaxation energy calculations indicate energy decreases of 0.0082 eV/Å$^2$, 0.0025 eV/Å$^2$, and 0.0093 eV/Å$^2$, respectively, for the three potentials, where the changes in the surface energies due to relaxations are in the order of 0.1% and in good agreement with results from [93]. It is seen that these three potentials predict different structures for the relaxed configuration. Note that the structures predicted by the SC and B potentials have the shortest and longest ranges of distortion, respectively.

### 3.4. Example 3: $\Sigma(5)$ symmetric twin boundary in fcc copper

It is known that grain boundary energy plays a key role in many interface related phenomena [71]. In order to calculate the grain boundary energies using atomistic models, it is necessary to understand the atomistic structure of grain boundaries. This has been the subject of many experimental and theoretical investigations [84,13,64,10].

Using the symmetry reduction idea, one can calculate the relaxed configuration of a grain boundary efficiently and fast. Among all the grain boundaries, one of the most studied ones is the $\Sigma(5)(2\,1\,0)[0\,0\,1]$ tilt boundary in fcc metals [9], where $\Sigma$ is the reciprocal density of coincidence sites. We calculate the relaxed configuration of atoms close to a symmetric $\Sigma(5)$ tilt boundary using all the three EAM potentials. The first step, similar to the previous examples, is to construct the reference configuration of the material body. Reference configuration was obtained by rotating two perfect copper crystals by a relative angle of 53.13° along their (001) axis while initially their (100) surfaces were facing each other. As it can be seen in Fig. 7a the grain boundary plane is a mirror plane of symmetry.

The atoms in the reference configuration are classified similar to the surface defect problem according to their distances from the twin boundary, which reduces the 3-D problem to a 1-D problem. In the twin boundary problem, atoms of the same class have displacement vectors with components both parallel ($y$-direction) and perpendicular ($x$-direction) to the twin boundary. The relaxation method is similar to the method used in the free surface problem, i.e., we use the simultaneous harmonic relaxation method. The iterations will continue until all forces have absolute values smaller than a force tolerance. In the relaxation process, the crystal is divided into two regions I and II. In Region I, atoms are relaxed individually, while atoms of Region II have no individual movements; they act as rigid blocks of ideal crystal structure free to translate in both directions.

*Numerical results.* We construct the material body in the reference configuration with 29 atomic layers in Region I. This means that one of the 29 layers lies on the grain boundary and would have only displacements parallel to the grain boundary and 14 layers on each side of the grain boundary that move in the (001) plane and their displacements are symmetric with respect to the grain

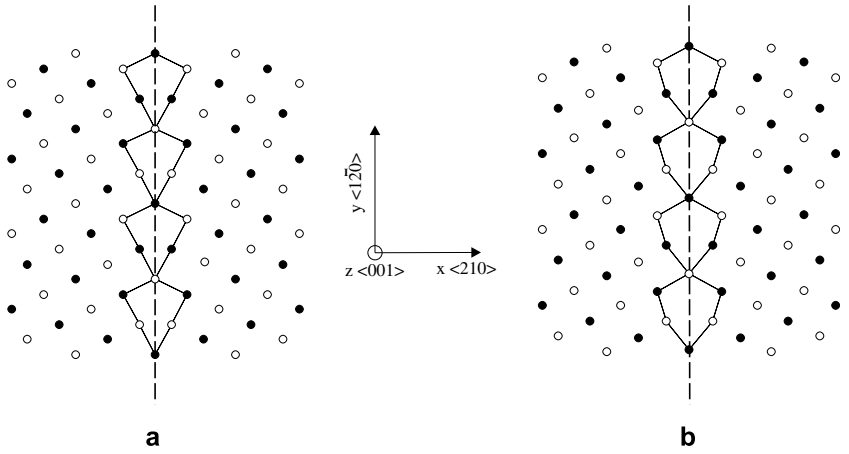


**Fig. 7.** Projection along the tilt axis of the structure of $\Sigma(5)(2\,1\,0)[0\,0\,1]$ grain boundary. (a) Atomic arrangements around the grain boundary in the reference configuration, (b) distortion of the atoms around the boundary after relaxation (white and dark circles correspond to two (001) planes).

boundary. We use all the three potentials to relax the atoms from their reference configuration. Fig. 7b shows atomic distortions in the vicinity of the grain boundary obtained by QSC potential.

Fig. 8 shows the displacements of the atomic layers in both directions. The relaxation energy per unit area of the grain boundary for each potential is calculated as 0.432002 eV/Å$^2$ using the SC Potential, 0.573276 eV/Å$^2$ using the QSC potential, and 0.0332358 eV/Å$^2$ using the B potential. It is seen that energy of the grain boundary strongly depends on the choice of the potential. Also both SC and QSC potentials are showing the same range of atomic distortions (atoms on the grain boundary and the first 10 closest layers from the grain boundary), while the result from B potential shows a longer range of atomic distortions (atoms on the grain boundary and the first 13 closest layers from the grain boundary).

### 3.5. Example 4: grain boundary in shape memory alloy NiAl

The NiAl compound has been of great interest to many material scientists because of its outstanding physical, chemical and mechanical properties which make it a promising material for high-temperature applications [96,73,76]. However, the exploitation of NiAl like many other intermetallic compounds is obstructed by its severe brittleness, which is believed to be due to the intrinsic brittleness of its grain boundaries. This explains the intense interest in grain boundaries in NiAl in the computational physics literature in recent years. Here, as another example, we calculate the atomic distortions in the vicinity of $\Sigma(5)(2\,1\,0)[0\,0\,1]$ symmetric tilt grain boundary for NiAl for both Ni-centered and Al-centered grain boundaries.

The method of solution is exactly the same as used in the solution of the $\Sigma(5)(2\,1\,0)[0\,0\,1]$ symmetric tilt boundary problem in fcc copper. First, we construct a reference configuration for $\Sigma(5)(2\,1\,0)[0\,0\,1]$ symmetric tilt GB using geometrical rules of the coincidence site lattice (CSL) model [85]. The (210) crystallographic plane is first aligned parallel to the intended grain boundary, and then a one-half crystal is rotated 180° relative to the other half crystal about the grain boundary normal. Similar to the problem of $\Sigma(5)(2\,1\,0)[0\,0\,1]$ symmetric tilt boundary in fcc copper, we divide the reference configuration into two regions: Region I contains atoms in the vicinity of the grain boundary which are allowed to move in two directions individually, while the atoms in Region II form a slab and move rigidly. Atoms of Region II serve to insure that the effect of the free surfaces on the relaxation of the atoms in Region I can be negligible. Atoms in Region II are constrained in their perfect lattice positions and are allowed to move as two rigid slabs.

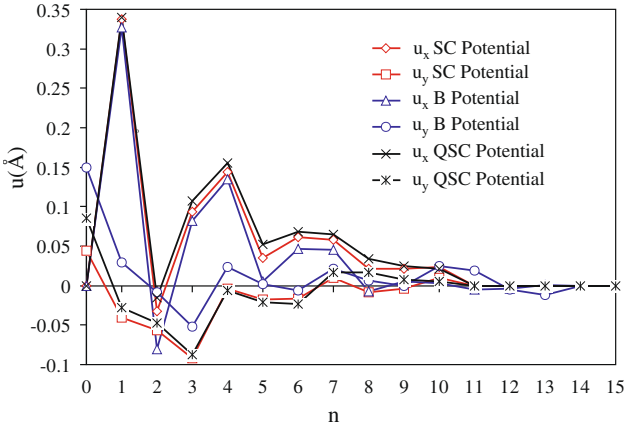


**Fig. 8.** Atomic displacements (Å) in the $x$ and $y$ directions close to the $\Sigma(5)(2\,1\,0)[0\,0\,1]$ tilt boundary.

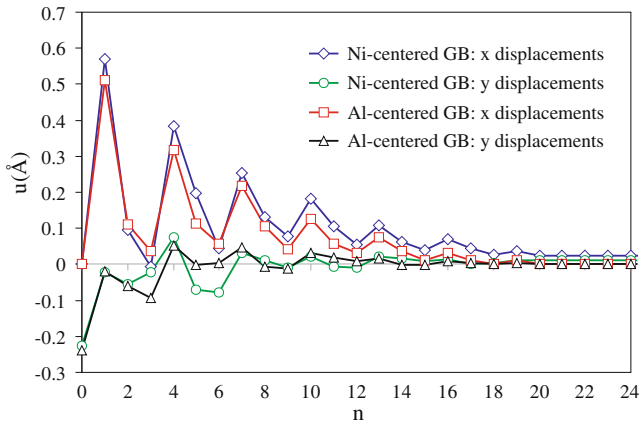


**Fig. 9.** Atomic displacements (Å) in the x and y directions close to Al-centered and Ni-centered $\Sigma(5)(2\,1\,0)[0\,0\,1]$ symmetric tilt grain boundaries in NiAl. For Al-centered GB, indices $n = 0,2,4,\ldots$ are occupied by Al atoms and indices $n = 1,3,\ldots$ are occupied by Ni atoms. Similarly, in the Ni-centered GB, indices $n = 0,2,4,\ldots$ are occupied by Ni atoms and indices $n = 1,3,\ldots$ are occupied by Al atoms.

*Numerical results.* The atomic distortions are calculated for both Ni-centered and Al-centered grain boundaries. Fig. 9 shows the displacements of the atomic layers for both cases. For Al-centered GB, indices $n = 0,2,4,\ldots$ are occupied by Al atoms and indices $n = 1,3,\ldots$ are occupied by Ni atoms. Similarly, in the Ni-centered GB, indices $n = 0,2,4,\ldots$ are occupied by Ni atoms and indices $n = 1,3,\ldots$ are occupied by Al atoms. We also calculated the relaxation energy of $-6.05641$ eV/Å$^2$ for Ni-centered grain boundary and $-14.3534$ eV/Å$^2$ for Al-centered grain boundary.

## 4. Conclusions

In this paper, we presented a formulation of anharmonic lattice statics for analysis of defective crystals with many-body interactions. This formulation is able to handle different types of defects with taking into account the anharmonic effects. This method is capable of generating semi-analytic solutions for defects (with partial symmetries) at zero temperature. Exploiting partial symmetries of defective crystals makes this method efficient and fast. As demonstrating examples, we used the method for three types of defects in fcc Cu, namely point defects, (001) free surfaces and $\Sigma(5)$ symmetric twin boundaries. We also looked at grain boundaries in the shape memory alloy NiAl.

It is well known that the structure and energy of a defect, in general, depend on the choice of potentials and we demonstrated this for fcc Cu, using three different EAM-type potentials. Therefore, in this sense, the method presented here can be used as a tool for comparing different interatomic potentials. We also observed that the choice of force tolerance can affect the predicted structures away from defects. We clearly observed this in the case of a point defect in fcc Cu.

As a future extension of this method, we will consider finite temperatures in a generalized lattice dynamics formulation. Such a formulation will be very useful in thermodynamic analysis of defective crystals at low temperatures, where MD cannot be used. This will be the subject of a future communication. We will also consider extending these ideas to more complicated situations, e.g. objective structures [49].

## References

[1] R.P. Agarwal, Difference Equations and Inequalities, Marcel Dekker, 2000.
[2] R.E. Allen, F.W. Dewette, Physical Review 179 (3) (1969) 873–886.
[3] R.E. Allen, F.W. Dewette, Physical Review 179 (3) (1969) 887–891.

[4] I. Babůska, E. Vitasek, F. Kroupa, Journal of Physics B 10 (1960) 419–427.
[5] I. Babůska, E. Vitasek, F. Kroupa, Journal of Physics B 10 (1960) 488–504.
[6] G.D. Barrera, R.H. de Tendler, E.P. Isoardi, Modelling and Simulation in Materials Science and Engineering B 8 (2000) 389–401.
[7] R. Benedek, Journal of Physics F-Metal Physics 8 (6) (1978) 1119–1129.
[8] K. Bennemann, Physical Review 124 (3) (1961) 669–670.
[9] F. Berthier, B. Legrand, G. Treglia, Interface Science 8 (1) (2000) 55–69.
[10] W. Bollmann, Philosophical Magazine 16 (140) (1967) 363.
[11] F. Bonneton, M. Drechsle, Surface Science 22 (2) (1970) 426.
[12] M. Born, K. Huang, Dynamical Theory of Crystal Lattices, Oxford University Press, 1988.
[13] A. Bourret, J.L. Rouviere, J.M. Penisson, Acta Crystallographica Section A 44 (1988) 838–847.
[14] L.L. Boyer, J.R. Hardy, Philosophical Magazine 24 (189) (1971) 647.
[15] M. Charlotte, L. Truskinovsky, Journal of the Mechanics and Physics of Solids 50 (2002) 217–251.
[16] J.H. Cho, Ismail, Z.Y. Zhang, E.W. Plummer, Physical Review B 59 (3) (1999) 1677–1680.
[17] A. Corciove, M. Croitoru, D. Grecu, Surface Science 21 (1) (1970) 109.
[18] H.L. Davis, J.R. Noonan, Journal of Vacuum Science and Technology 20 (3) (1982) 842–845.
[19] H.L. Davis, J.R. Noonan, Surface Science 126 (1–3) (1983) 245–252.
[20] M.S. Daw, S.M. Foiles, M.I. Baskes, Materials Science Reports 9 (1992) 251–310.
[21] M.S. Daw, M.I. Baskes, Physical Review B 29 (12) (1984) 6443–6453.
[22] Ph. Dederich, G. Leibfrie, Physical Review 188 (3) (1969) 1175–1183.
[23] P.H. Dederichs, C. Lehmann, H.R. Schober, A. Scholz, R. Zeller, Journal of Nuclear Materials 69-7 (1–2) (1978) 176–199.
[24] S.N. Elaydi, An Introduction to Difference Equations, Springer, 1996.
[25] F. Ercolessi, M. Parrinello, E. Tosatti, Philosophical Magazine A-Physics of Condensed Matter Structure Defects And Mechanical Properties 58 (1) (1988) 213–226.
[26] J.D. Eshelby, Journal of Applied Physics 25 (2) (1954) 255–261.
[27] J.D. Eshelby, Acta Metallurgica 3 (5) (1955) 487–490.
[28] Te. Feuchtwa, Physical Review 155 (3) (1967) 715–730.
[29] M.W. Finnis, J.E. Sinclair, Philosophical Magazine A-Physics of Condensed Matter Structure Defects and Mechanical Properties 50 (1) (1984) 45–55.
[30] J.W. Flocken, J.R. Hardy, Physical Review 175 (3) (1968) 919–927.
[31] J.W. Flocken, J.R. Hardy, Physical Review 177 (3) (1969) 1054–1062.
[32] J.W. Flocken, J.R. Hardy, Physical Review B 1 (6) (1970) 2447–2456.
[33] J.W. Flocken, Physical Review B 2 (6) (1970) 1743–1752.
[34] J.W. Flocken, Physical Review B 4 (4) (1971) 1187–1196.
[35] J.W. Flocken, Physical Review B 6 (4) (1972) 1176–1181.
[36] J.W. Flocken, Physical Review B 9 (12) (1974) 5133–5143.
[37] J.W. Flocken, Physical Review B 15 (8) (1977) 4132–4135.
[38] D.C. Gazis, R.F. Wallis, Surface Science 3 (1965) 19–32.
[39] L.A. Girifalco, J.R. Streetman, Journal of Physics and Chemistry of Solids 4 (3) (1958) 182–189.
[40] L.A. Girifalco, V.G. Weizer, Journal of Physics and Chemistry of Solids 12 (3–4) (1960) 260–264.
[41] G. Grochola, S.P. Russo, I. Yarovsky, I.K. Snook, Journal of Chemical Physics 120 (7) (2004) 3425–3430.
[42] G.L. Hall, Journal of Physics and Chemistry of Solids 3 (3–4) (1957) 210–222.
[43] U. Hansen, P. Vogl, V. Fiorentini, Physical Review B 60 (7) (1999) 5055–5064.
[44] J.R. Hardy, Journal of Physics and Chemistry of Solids 29 (11) (1968) 2009–2014.
[45] J.R. Hardy, J.W. Flocken, Physical Review 175 (1968) 919–927.
[46] B. Houchmandzadeh, J. Lajzerowicz, E. Salje, Journal of Physics-Condensed Matter 4 (49) (1992) 9779–9794.
[47] E.P. Isoardi, N.L. Allan, G.D. Barrera, Physical Review B 69 (2004) 024303.
[48] D.P. Jackson, Canadian Journal of Physics 49 (16) (1971) 2093–2097.
[49] R.D. James, Journal of the Mechanics and Physics of Solids 54 (2006) 2354–2390.
[50] R.A. Johnson, Physical Review A-General Physics 134 (5A) (1964) 1329–1339.
[51] R.A. Johnson, Physical Review 145 (2) (1966) 423–433.
[52] R.A. Johnson, Physical Review B 27 (4) (1983) 2014–2018.
[53] R.A. Johnson, E. Brown, Physical Review 127 (2) (1962) 446–454.
[54] R.A. Johnson, A.C. Damask, G.J. Dienes, Acta Metallurgica 12 (11) (1964) 1215–1224.
[55] H. Kanzaki, Journal of Physics and Chemistry Of Solids 2 (1) (1957) 24–36.
[56] H. Kanzaki, Journal of Physics and Chemistry of Solids 2 (2) (1957) 107–114.
[57] M. Karimi, M. Mostoller, Physical Review B 45 (11) (1992) 6289–6292.
[58] A.M. Karo, J.R. Hardy, Physical Review B 3 (10) (1971) 3418–3425.
[59] H.H. Kart, M. Tomak, T. Cagin, Modelling and Simulation in Materials Science and Engineering 13 (5) (2005) 657–669.
[60] O. Kastner, Continuum Mechanics and Thermodynamics 15 (2003) 487–502.
[61] S. Kato, Japanese Journal of Applied Physics 13 (2) (1974) 218–222.
[62] S. Kohlhoff, P. Gumbsch, H.F. Fischmeister, Philosophical Magazine A 64 (1968) 851–878.
[63] L.S. Kothari, C.M. Singal, Physical Review 168 (3) (1968) 952–956.
[64] M.L. Kronberg, F.H. Wilson, Transactions of the American Institute of Mining and Metallurgical Engineers 185 (8) (1949) 501–514.
[65] V. Lakshmikantham, D. Trigiante, Theory of Difference Equations: Numerical Methods and Applications, Academic Press, 1983.
[66] U. Landman, R.N. Hill, M. Mostoller, Bulletin of the American Physical Society 25 (3) (1980) 234.
[67] D.M. Lind, F.B. Dunning, G.K. Walters, H.L. Davis, Physical Review B 35 (17) (1987) 9037–9044.
[68] W.K. Liu, E.G. Karpov, S. Zhang, H.S. Park, Computer Methods in Applied Mechanics and Engineering 193 (17-20) (2004) 1579–1601.
[69] A.H. Love, Mathematical Theory of Elasticity, Cambridge University Press, Cambridge, England, 1924.
[70] J.E. Marsden, T.J.R. Hughes, Mathematical Foundations of Elasticity, Dover, New York, 1983.
[71] S.P. Marsh, C.S. Pande, Modeling of Coarsening and Grain Growth, TMS, Warrendale, PA, 1993.
[72] R. Mayer, C.S. Zhang, K.G. Lynn, W.E. Frieze, F. Jona, P.M. Marcus, Physical Review B 35 (7) (1987) 3102–3110.
[73] D.B. Miracle, Acta Metallurgica et Materialia 41 (3) (1993) 649–684.
[74] M. Mostoller, R.M. Nicklow, D.M. Zehner, S.C. Lui, J.M. Mundenar, E.W. Plummer, Physical Review B 40 (5) (1989) 2856–2872.
[75] T. Ning, Q.L. Yu, Y.Y. Ye, Surface Science 206 (1–2) (1988) L857–L863.
[76] R.D. Noebe, R.R. Bowman, M.V. Nathal, International Materials Reviews 38 (4) (1993) 193–232.
[77] N.I. Papanicolaou, H. Chamati, G.A. Evangelakis, D.A. Papaconstantopoulos, Computational Materials Science 27 (1–2) (2003) 191–198.
[78] H. Rafiitabar, A.P. Sutton, Philosophical Magazine Letters 63 (4) (1991) 217–224.
[79] S. Rao, C. Hernandez, J.P. Simmons, T.A. Parthasarathy, C. Woodward, Philosophical Magazine A 77 (1) (1998) 231–256.
[80] A.M. Rodriguez, G. Bozzolo, J. Ferrante, Surface Science 289 (1–2) (1993) 100–126.
[81] N.M. Sergey, E.G. Karpov, W.K. Liu, Journal of Computational Physics 218 (2006) 836–859.
[82] J.E. Sinclair, P.C. Gehlen, R.G. Hoagland, J.P. Hirth, Journal of Applied Physics 4 (7) (1978) 3890–3897.
[83] I. Stakgold, Quarterly of Applied Mathematics 8 (1950) 169–186.
[84] A.P. Sutton, R.W. Balluffi, Acta Metallurgica 35 (9) (1987) 2177–2201.
[85] A.P. Sutton, R.W. Balluffi, Interfaces in Crystalline Materials, Oxford Science Publication, New York, 1995.
[86] A.P. Sutton, J. Chen, Philosophical Magazine Letters 61 (3) (1990) 139–146.
[87] E.B. Tadmor, M. Ortiz, R. Philips, Philosophical Magazine A 73 (1996) 1529–1563.
[88] V.K. Tewary, Proceedings of the Physical Society of London 92 (578P) (1967) 987–989.
[89] V.K. Tewary, R. Bullough, Journal of Physics F-Metal Physics 1 (5) (1971) 554–569.
[90] V.K. Tewary, Advances in Physics 22 (6) (1973) 757–810.
[91] L. Tewordt, Physical Review 109 (1) (1958) 61–68.
[92] R.F. Wallis, B.C. Clark, R. Herman, Physical Review 167 (3) (1968) 652–658.
[93] J. Wan, Y.L. Fan, D.W. Gong, S.G. Shen, X.Q. Fan, Modelling and Simulation in Materials Science and Engineering 7 (2) (1999) 189–206.
[94] P. Wynblatt, N.A. Gjostein, Surface Science 22 (1) (1970) 125–136.
[95] P. Wynblatt, N.A. Gjostein, Surface Science 12 (2) (1968) 109–127.
[96] X. Xie, Y. Mishin, Acta Materialia 50 (17) (2002) 4303–4313.
[97] A. Yavari, M. Ortiz, K. Bhattacharya, Journal of Elasticity 86 (2007) 41–83.
[98] A. Yavari, M. Ortiz, K. Bhattacharya, Philosophical Magazine 87 (26) (2007) 3997–4026.
[99] A. Yavari, A. Ozakin, Zeitschrift für Angewandte Mathematik und Physik (ZAMP), 2008. doi:10.1007/s00033-007-7127-2.
[100] A. Yavari, J.E. Marsden, Zeitschrift für Angewandte Mathematik und Physik (ZAMP), in press, doi:10.1007/s00033-008-8059-1.
[101] J.M. Zhang, F. Ma, K.W. Xu, Surface and Interface Analysis 35 (8) (2003) 662–666.
[102] J.M. Zhang, K.W. Xu, F. Ma, Acta Physica Sinica 52 (8) (2003) 1993–1999.
[103] J.M. Zhang, F. Ma, K.W. Xu, Applied Surface Science 229 (1–4) (2004) 34–42.